Tropical Journal of Pharmaceutical Research August 2019; 18 (8): 1635-1641
ISSN: 1596-5996 (print); 1596-9827 (electronic)

Available online at http://www.tjpr.org
http://dx.doi.org/10.4314/tjpr.v18i8.10

Original Research Article

Substructural dynamics of the phase-I drug metabolizing enzyme, carbonyl reductase 1, in response to various substrate and inhibitor configurations

Mahmoud Kandeel[1,2]*, Abdulla Al-Taher[1], Mohammed Al-Nazawi[1], Kantaro Oh-hashi[3,4]

[1]Department of Physiology, Biochemistry, and Pharmacology, College of Veterinary Medicine, King Faisal University, 31982 Al-Ahsa, Saudi Arabia, [2]Department of Pharmacology, Faculty of Veterinary Medicine, Kafrelsheikh University, 33516 Kafrelsheikh, Egypt, [3]Department of Chemistry and Biomolecular Science, Faculty of Engineering, [4]United Graduate School of Drug Discovery and Medical Information Sciences, Gifu University, 1-1 Yanagido, Gifu 501-1193, Japan

For correspondence: **Email: mkandeel@kfu.edu.sa; **Tel:** +966-568918734*

Sent for review: 19 April 2019 *Revised accepted: 25 July 2019*

Abstract

Purpose: *To investigate the substructure and molecular dynamics change in the phase-I drug metabolizing enzyme, carbonyl reductase 1 (CBR1), in response to different substrate and inhibitor configurations, using a molecular dynamics approach.*

Methods: *CBR1 structure and drug ligands, including 2,3-butanedione, prostaglandin E2 (PGE2), oracine, mitoxantrone, menadione, rutoside, barbital, and biochanin A, were retrieved and 3D optimized. Docking runs were performed using template docking into CBR1 active binding site with GSH. Molecular dynamic (MD) simulation was implemented for 100 ns.*

Results: *The docking scores were positively correlated with the detected ligand's affinities. Molecular dynamics simulation indicated that lower affinity ligands or weaker inhibitors produced less stable CBR1 with higher root mean square deviations (RMSD) of CBR1 backbone α-carbon atoms. Stronger inhibitors and substrates produced stable CBR1 structures with RMSD similar to or lower than CBR1-NADP complexes. Very low affinity ligands were unstable and were released from their sites within a few nanoseconds after commencing the simulation. Two flexible loops, LE92-PHE102 and VAL230-TYR251, were highly responsive to the nature of CBR1 ligands. Changes in the latter may be associated with lower CBR1 activity due to loss of stabilization of NADPH by the deviation of this loop's residues.*

Conclusion: *In this work, a model of CBR1 structural changes has been provided that can be used in the analysis of CBR1 future substrates and inhibitors. Docking followed by MD simulation and analysis of average backbone α-carbon RMSD and changes in ILE92-PHE102 and VAL230-TYR251 loops can be used in the model analysis of unknown or new drug candidates to predict their binding efficiencies.*

Keywords: *Carbonyl reductase, Phase-1 metabolism, Molecular dynamics, Docking*

Tropical Journal of Pharmaceutical Research is indexed by Science Citation Index (SciSearch), Scopus, International Pharmaceutical Abstract, Chemical Abstracts, Embase, Index Copernicus, EBSCO, African Index Medicus, JournalSeek, Journal Citation Reports/Science Edition, Directory of Open Access Journals (DOAJ), African Journal Online, Bioline International, Open-J-Gate and Pharmacy Abstracts

INTRODUCTION

Carbonyl reductase 1 (CBR1, E.C. 1.1.1.184) is a member of a large family of short-chain reductases/dehydrogenases. They are required for detoxification of compounds bearing carbonyl groups, including a wide range of drugs, toxins, chemicals, and xenobiotics [1]. Besides, CBR1

shows marked activity toward endogenous carbonyl substrates such as eicosanoids and steroids [2]. Carbonyl reductase 1 increases the toxicity of the anticancer anthracycline doxorubicin by producing less active and more toxic alcoholic derivatives. Also, CBR1 overexpression in cancer cells has been associated with drug resistance against treatment with anthracycline anticancer drugs [3]. There are two highly homologous isoforms of CBRs in humans, CBR1 and CBR3. Furthermore, the catalytic efficiency of CBR1 was much higher than its isoform CBR3 [4]. Therefore, CBR1 is considered as the most critical CBR in phase-I metabolism of drugs.

CBR1 has a wide range of substrate specificity. Yet, the exact molecular basis of this high specificity is still not well understood. Molecular dynamics simulation explores protein-ligand interactions and delivers useful *in situ* structural responses that cannot be easily reached by other techniques. A plausible binding model can be suggested after comprehensive testing of initial docking configuration followed by a brief MD experiment. During docking studies, the ligand is kept flexible and docked against a fixed protein geometry [5]. To account for protein flexibility, MD simulation contributes to the understanding of the mechanisms underlying substrate recognition by CBR1.

To evaluate the interactions of several ligand configurations with CBR1, several CBR1 substrates and inhibitors with various structures and biological activities were selected (Figure 1). The selected drugs and toxins contain carbonyl moieties and proved to be substrates or inhibitors for CBR1, including 2,3-butanedione, barbital, biochanin A, prostaglandin E2 (PGE2), oracin, mitoxantrone, and menadione. 2,3-butanedione is a diacetyl and is used as flavoring agents in food, electronic cigarettes, and alcoholic beverages [6,7].

Barbital was discovered a century ago and was used as a hypnotic agent [8]. Biochanin A is an O-methylated isoflavone and was found to inhibit CBR1 at a level of 2 µM [9]. Prostaglandin E2 is a substrate for CBR1 with K_m value of 0.1 mM [10]. Oracin an anti-proliferative agent and a substrate for CBR1 with K_m value of 96 µM [11]. Mitoxantrone is a less toxic antineoplastic agent related to doxorubicin. It has chemical modifications that prohibit rapid metabolism by CBR1, resulting in lower cardiotoxicity [12]. Menadione is a chemical compound with vitamin K activity with moderate affinity to CBR1 and K_m value of 42 µM [13].

METHODS

Collection, preparation, and optimization of drug structures

The compounds shown in Figure 1 were searched, and their 2D structures were downloaded from the PubChem database. The 2D structure was desalted, cleaned, energy minimized, and 3D optimized by Ligprep software. The optimized structures at neutral pH were saved as SDF files.

CBR1 structure preparation

The protein data bank was searched to retrieve CBR1 bound to GSH (PDB ID 4Z3D). The binding coordinates of GSH were used to conclude the docking sites for the tested drugs. Water and other crystallographic molecules were removed. The protein side chains and missing atoms were corrected. Non-polar hydrogens were added, and the whole structure was energy minimized to remove any structure deformities or clashes before the docking started.

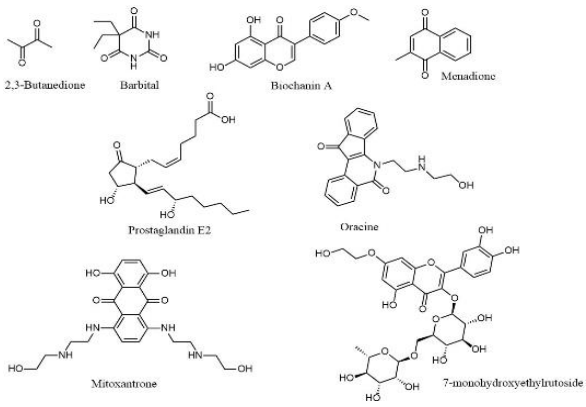

Figure 1: Structure of drugs used in this study

Docking

The docking strategy, evaluation, validation, and selection of best configurations were performed as previously described [20]. The important benchmarks were the distance of the carbonyl group from the C4 atom of NADPH and the proximity of the carbonyl oxygen to TYR193. The shorter distance between the carbonyl group and the C4 atom of NADPH ensures efficient hydride transfer, and tyrosine residue acts as a proton donor. Molegro Virtual Docker (MVD) 5.5 software was used to dock the drugs into CBR1 active site. MolDock was selected as a scoring function. The docking template was built on GSH binding coordinates. A docking space of 15 Å around the template position was used. A maximum of 10 poses were generated. Docking

validity was confirmed by the re-docking of GSH. Complementarity of the docked GSH with its position in the co-crystallized structure indicated the efficacy of docking runs.

Molecular dynamics studies of CBR1

Molecular dynamics changes and structure responses of CBR1 to different ligands were assessed by MD simulation for 100 ns. YASARA software (version 14.12.2) was used in all MD simulations. The force field used was AMBER14. Long-range electrostatic forces were handled using Particle-mesh Ewald algorithm [21]. The enzyme was soaked in a simulation cell with water density of 0.997 g/mL, and boundaries were kept at about 10 Å around the protein. Counter ions were added to simulate physiological conditions. Isothermal (298K) and isobaric conditions (NPT ensemble) were maintained throughout the simulation time. Steepest descent minimization was used to prime the structure preparation. Time step was set to 2 fs, and simulation snapshots were collected every 100 ps. After the end of the simulation, the average structure file was generated and used to compare changes in CBR1.

Other molecular modeling methods

Production of figures and inspection and handling of molecular structure files were done using several software packages, including ICM molsoft, Maestro, Microsoft Excel, and GraphPad Prism software.

RESULTS

Molecular docking

The docked compounds showed docking scores ranging from -150 to -550 (Table 1). There was a positive correlation between the obtained k_m values and the detected docking score (r = 0.62). Substrates with higher k_m are more likely to get higher docking score. Larger size ligands showed higher docking scores as well as lower k_m values, indicating stronger binding with CBR1. Mitoxantrone, which is a lower affinity substrate compared to doxorubicin, showed lower docking score compared to doxorubicin, oracine, and PGE2. This indicates the validity of the docking run, which correlates with the previous reports, indicating the lower affinity of mitoxantrone to CBR1 when compared to doxorubicin [17]. The strong inhibitors, biochanin A and rutoside, showed high docking scores of -532 and -550 respectively. They were associated with their low Ki values in the low micromolar range (Table 1).

CBR1-drug interactions

During docking runs, a template was generated from the coordinates of GSH interaction. Figure 2 shows the interactions of selected drugs with CBR1. The carbonyl groups were efficiently docked near the catalytic residues, SER139 and TYR193.

Structural stability of CBR1-drug complexes

The changes in RMSDs of CBR1 α-carbon atoms during recognition of different compound configurations were monitored for 100 ns in several MD simulation runs (Figure 3 and 4). The average distance of the backbone α-carbon was calculated by comparing the positions of atoms during MD simulations. According to the obtained average RMSD values, the drugs can be classified into three groups. The first group comprised drugs with slightly higher RMSD when compared to Apo-CBR1 and included PGE2 and rutoside (Figure 3 B). The second group showed lower RMSD values compared to Apo-CBR1 and included 2,3-butanedione, barbital, biochanin A, mitoxantrone, and menadione (Figure 4 A). The third group had extremely low RMSD value as

Table 1: Substrate and inhibitor potencies of the compounds used in this study and their associated docking scores and hydrogen bonding

Variable	Substrate K_m (mM)	Inhibitor K_i (mM)	Reference	Docking score	H-bond energy
2,3-Butanedione	1.8	--	[14]	-150	-2.3
PGE2	0.1	--	[14]	-501	-10.2
Oracine	0.096	--	[15]	-372	-1.6
Doxorubicin	0.09	--	[16,17]	-499	-15.2
Mitoxantrone	0.2	--	[17]	-457	-11.4
Menadione	0.018	--	[11]	-237	0
Rutoside	--	0.033	[18]	-550	-20
Barbital	--	18% at 1mM	[19]	-245	-2.3
Biochanin A	--	0.00203	[9]	-532	-9.2

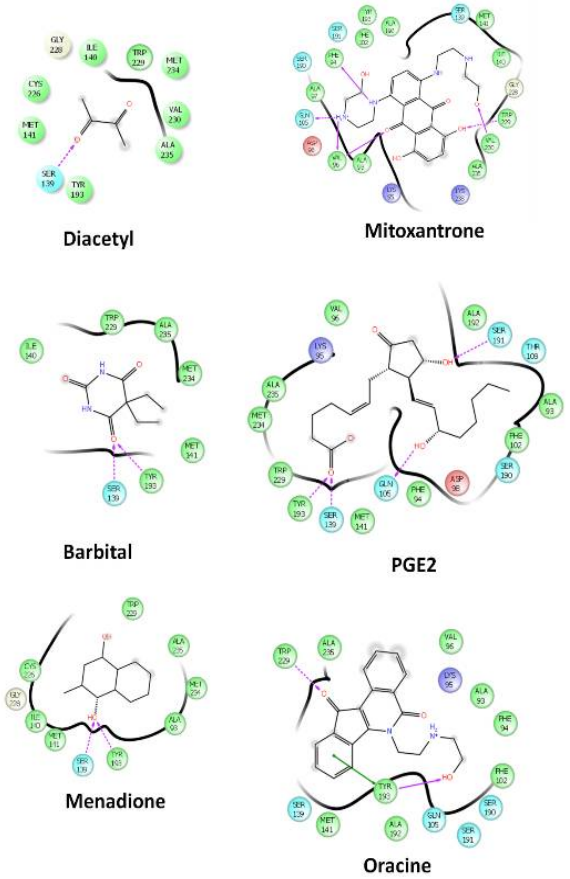

Figure 2: The docking site and interactions of diacetyl, mitoxantrone, barbital, PGE2, menadione, and oracine with CBR1

2,3-butanedione, barbital, and menadione (Figure 4 B).

Rutoside and PGE2 showed rapidly stabilized RMSD within 20 ns with slightly higher RMSD at the start of the simulation and extended for 85 ns when compared to CBR1 bound to NADP without any other substrate (ApoCBR1). ApoCBR1 (CBR1 without substrate) was less stable than CBR1-PGE2 and CBR1-rutoside due to RMSD fluctuation during 100 ns simulation (Figure 3B). The average α-carbon RMSD values were 1.88, 2, and 1.94 Å for ApoCBR1, CBR1-PGE2, and CBR1-rutoside, respectively.

Biochanin A and mitoxantrone showed an average RMSD change of 1.6 Å, which is 0.22 Å lower than ApoCBR1. The lowest MW compounds, barbital and 2,3-Butanedione, showed the lowest average RMSD, which were 1.3 and 1.5 Å respectively.

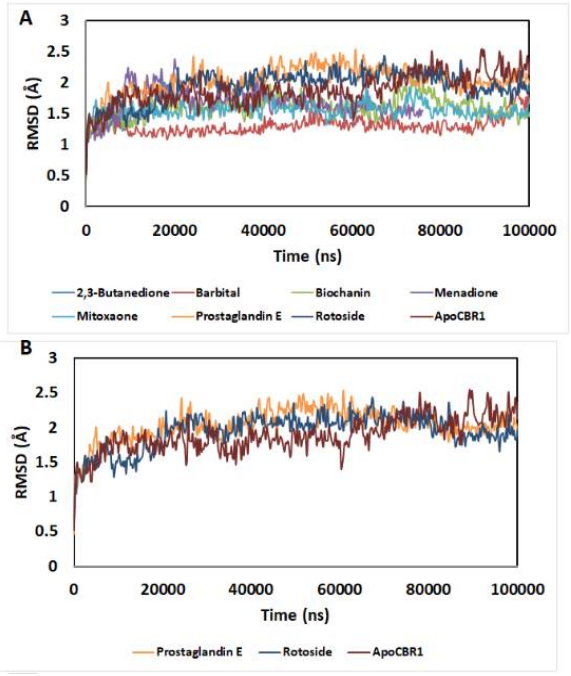

Figure 3: RMSD of the α-carbon atom in the CBR1 structures during 100 ns of MD simulation. (A) ApoCBR1: CBR1 bound to NADP or CBR1 bound with different ligands, (B) ApoCBR1: CBR1 bound to NADP or CBR1 bound with PGE2 or rutoside,

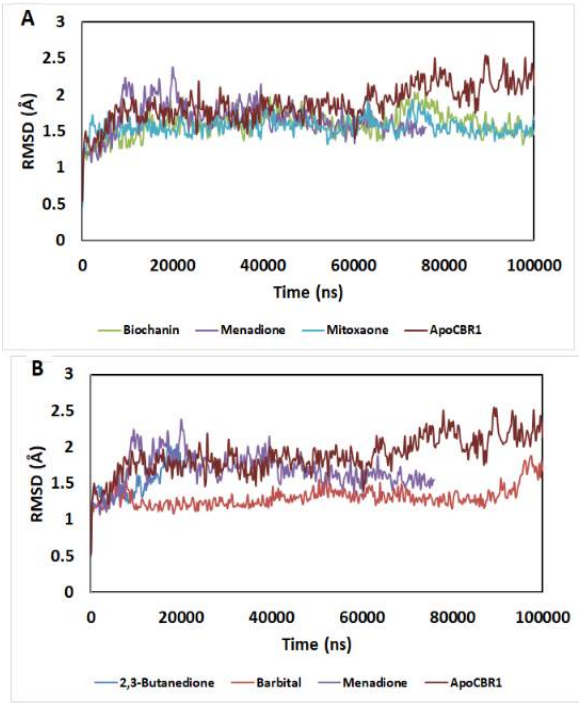

Figure 4: RMSD of the α-carbon atom in the CBR1 structures during 100 ns of MD simulation. (A) ApoCBR1: CBR1 bound to NADP or CBR1 bound to biochanin, menadione or mitoxantrone, (B) ApoCBR1: CBR1 bound to NADP or CBR1 bound with 2,3-butanedione or barbital

Substructure and residual changes in CBR1

Within the CBR1 structure, two regions were the most responsive for the nature of binding ligands. The first was the flexible loop - ILE92-PHE102, while the second region is the VAL230-TYR251 loop (Figure 5 and 6), which contains residues that are important for binding of NADP as well as the substrate. Changes in RMSD in these two regions were dependent on the type of ligand bound with CBR1, which can be categorized into three groups. The first group comprised PGE2 and rutoside and showed a marked increase in RMSD in these two loops compared to ApoCBR1 (Figure 5 B). The second group did not show marked RMSD changes and comprised biochanin and mitoxantrone. The third group, 2,3-Butanediol, barbital, and oracine, produced lower RMSD changes in the two regions.

Instability of binding of low molecular weight ligands

The low mw ligands as 2,3-butanedione and menadione showed unstable binding with CBR1. Molecular dynamics experiments showed that the compounds were released from the active site within 10 ns from the start of the simulation. This was associated with lower RMSD changes in CBR1.

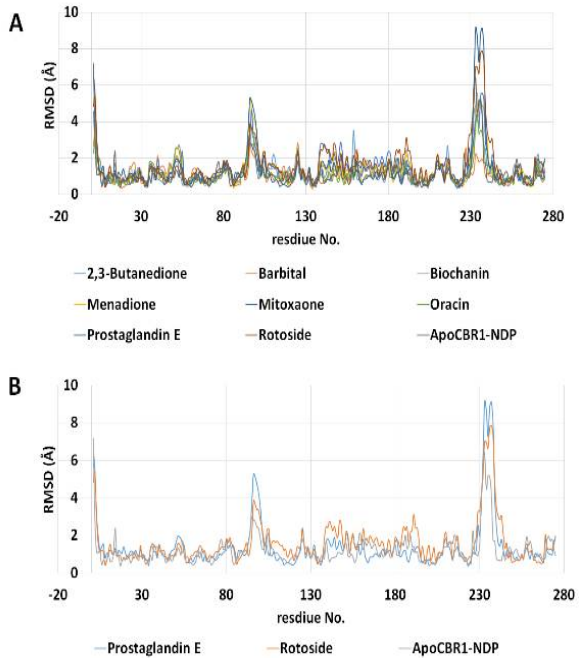

Figure 5: Per-residue RMSD of CBR1 structures during 100 ns of MD simulation. (A) ApoCBR1: CBR1 bound to NADP or CBR1 bound with different ligands, (B) ApoCBR1: CBR1 bound to NADP or CBR1 bound to PGE2 or rutoside

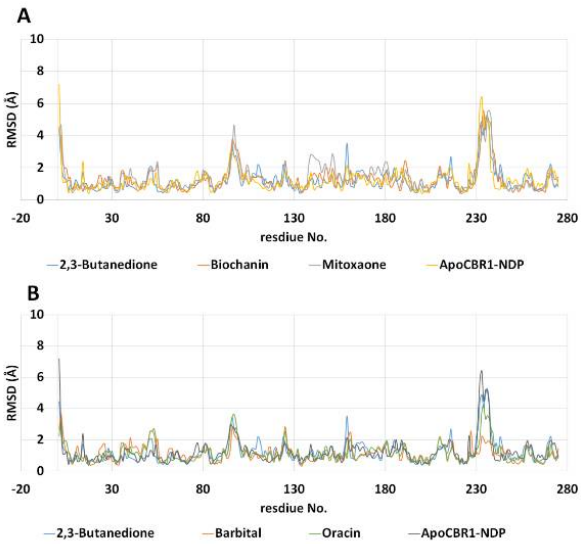

Figure 6: Per-residue RMSD of CBR1 structures during 100 ns of MD simulation. (A) ApoCBR1: CBR1 bound to NADP or CBR1 bound to biochanin, menadione or mitoxantrone, (B) ApoCBR1: CBR1 bound to NADP or CBR1 bound to 2,3-butanedione or barbital

DISCUSSION

A broad range of compounds, a feature that is less common in the short-chain dehydrogenase/reductase family [22]. Molecular dynamics simulation was used to identify structural changes in proteins in response to various interactions with smaller molecules or cellular components [23-25]. The flexibility of this technique allows for the identification of substructure responses in snapshots of time, a property that helps in understanding various molecular responses that cannot be easily identified by other techniques.

Carbonyl reductase 1 can metabolize PGE2, which is a fever mediator, to yield the less active PGF2α [13]. It is a medium affinity substrate with k_m = 100 µM. PGE2 showed high docking score equal to -501. The complex between CBR1 and PGE2 was less stable and showed higher RMSD changes during 100 ns of MD simulation. Also, PGE2 produced higher RMSD changes in the flexible loop, ILE92-PHE102, as well as in VAL230-TYR251 loop. These changes resulted in an outward deviation of important residues in the stabilization of NADPH. This may result in the lower affinity of PGE2.

In this study, two CBR1 inhibitors, rutoside and biochanin A, were evaluated. The former is a medium affinity inhibitor at 33 µM concentration, while the latter is a potent inhibitor at 2 µM levels [9,26]. Interestingly, biochanin A produced

favorable dynamics profile by stabilizing CBR1, which showed lower average structure RMSD and smaller changes in the two CBR1 flexible loops. In contrast, the weaker inhibitor, rutoside, showed less stable CBR1 and higher RMSD changes.

The poor affinity ligand, 2,3-butanedione (**K_m** = 1.8 mM, [14]), showed unstable binding with CBR1 that led to complete detachment from the active site within a few nanoseconds from the start of MD simulation. This is also supported by lower RMSD (Figure 3, 4) and lower RMSD in the VAL230-TYR251 loop.

The VAL230-TYR251 loop was the most responsive element in CBR1 structure, which is associated with the potency of the binding ligand. Conservation of this loop conformation in alignment with NDPH-bound conformation (ApoCBR1) was associated with stronger ligand binding pattern. The lower affinity ligands showed lower RMSD changes in this loop.

CONCLUSION

Molecular docking and MD simulation were used to develop a model for testing the recognition of ligands by CBR1. Higher RMSD in VAL230-TYR251 loop denotes deviation of the NDPH stabilizing structures that might favor poor CBR1 activity. Stabilization of this loop is associated with stronger binding ligands. The average backbone α-carbon RMSD and changes in ILE92-PHE102 and VAL230-TYR251 loops can be used in the model analysis of unknown new drug candidates and can be used as a tool to predict the potential interactions of existing drugs with CBR1.

DECLARATIONS

Acknowledgement

This work was supported by Deanship of Scientific Research under NASHIR track (Project no. 186028).

Conflict of interest

The authors declare that no conflict of interest is associated with this work.

Contribution of authors

We declare that the authors named in this article performed this work, and will bear all liabilities for claims related to the content of this article. MK and AA designed the experiment, MK carried out the experiment, MK wrote the paper, MA, KO revised the manuscript.

Open Access

REFERENCES

1. *El-Hawari Y, Favia AD, Pilka ES, Kisiela M, Oppermann U, Martin HJ, Maser E. Analysis of the substrate-binding site of human carbonyl reductases CBR1 and CBR3 by site-directed mutagenesis. Chem Biol Interact 2009; 178(1-3): 234-241.*
2. *Pilka ES, Niesen FH, Lee WH, El-Hawari Y, Dunford JE, Kochan G, Wsol V, Martin HJ, Maser E, Oppermann U. Structural basis for substrate specificity in human monomeric carbonyl reductases. PLoS One 2009; 4(10): e7113.*
3. *Gonzalez B, Akman S, Doroshow J, Rivera H, Kaplan WD, Forrest GL. Protection against daunorubicin cytotoxicity by expression of a cloned human carbonyl reductase cDNA in K562 leukemia cells. Cancer Res 1995; 55(20): 4646-4650.*
4. *Lal S, Sandanaraj E, Wong ZW, Ang PC, Wong NS, Lee EJ, Chowbay B. CBR1 and CBR3 pharmacogenetics and their influence on doxorubicin disposition in Asian breast cancer patients. Cancer Sci 2008; 99(10): 2045-2054.*
5. *Guedes IA, de Magalhaes CS, Dardenne LE. Receptor-ligand molecular docking. Biophys Rev 2014; 6(1): 75-87.*
6. *Pavia DL, Lampman GM, Engel RG, Kriz GS. Introduction to organic laboratory techniques: A microscale approach: Saunders college publishing New York; 1999.*
7. *Clapp PW, Jaspers I. Electronic Cigarettes: Their Constituents and Potential Links to Asthma. Curr Allergy Asthma Rep 2017; 17(11): 79.*
8. *Davalos JZ, Ribeiro da Silva M, Ribeiro da Silva MA, Freitas VL, Jimenez P, Roux MV, Cabildo P, Claramunt RM, Elguero J. Computational thermochemistry of six ureas, imidazolidine-2-one, N,N'-trimethyleneurea, benzimidazolinone, parabanic acid, barbital (5,5'-diethylbarbituric acid), and 3,4,4'-trichlorocarbanilide, with an extension to related compounds. J Phys Chem A 2010; 114(34): 9237-9245.*
9. *Zimmermann TJ, Niesen FH, Pilka ES, Knapp S, Oppermann U, Maier ME. Discovery of a potent and*

selective inhibitor for human carbonyl reductase 1 from propionate scanning applied to the macrolide zearalenone. Bioorg Med Chem 2009; 17(2): 530-536.

10. *Bohren KM, Wermuth B, Harrison D, Ringe D, Petsko GA, Gabbay KH. Expression, crystallization and preliminary crystallographic analysis of human carbonyl reductase. J Mol Biol 1994; 244(5): 659-664.*
11. *Hartmanova T, Tambor V, Lenco J, Staab-Weijnitz CA, Maser E, Wsol V. S-nitrosoglutathione covalently modifies cysteine residues of human carbonyl reductase 1 and affects its activity. Chem Biol Interact 2013; 202(1-3): 136-145.*
12. *Shee K, Kono AT, D'Anna SP, Seltzer MA, Lu X, Miller TW, Chamberlin MD. Maximizing the Benefit-Cost Ratio of Anthracyclines in Metastatic Breast Cancer: Case Report of a Patient with a Complete Response to High-Dose Doxorubicin. Case Rep Oncol 2016; 9(3): 840-846.*
13. *Gonzalez-Covarrubias V, Ghosh D, Lakhman SS, Pendyala L, Blanco JG. A functional genetic polymorphism on human carbonyl reductase 1 (CBR1 V88I) impacts on catalytic activity and NADPH binding affinity. Drug Metab Dispos 2007; 35(6): 973-980.*
14. *Bohren KM, Wermuth B, Harrison D, Ringe D, Petsko GA, Gabbay KH. Expression, crystallization and preliminary crystallographic analysis of human carbonyl reductase. J Mol Biol 1994; 244(5): 659-664.*
15. *Hartmanova T, Tambor V, Lenco J, Staab-Weijnitz CA, Maser E, Wsol V. S-nitrosoglutathione covalently modifies cysteine residues of human carbonyl reductase 1 and affects its activity. Chem Biol Interact 2013; 202(1-3): 136-145.*
16. *Kassner N, Huse K, Martin HJ, Godtel-Armbrust U, Metzger A, Meineke I, Brockmoller J, Klein K, Zanger UM, Maser E, Wojnowski L. Carbonyl reductase 1 is a predominant doxorubicin reductase in the human liver. Drug Metab Dispos 2008; 36(10): 2113-2120.*
17. *Slupe A, Williams B, Larson C, Lee LM, Primbs T, Bruesch AJ, Bjorklund C, Warner DL, Peloquin J, Shadle SE, Gambliel HA et al. Reduction of 13-deoxydoxorubicin and daunorubicinol anthraquinones by human carbonyl reductase. Cardiovasc Toxicol 2005; 5(4): 365-376.*
18. *Gonzalez-Covarrubias V, Kalabus JL, Blanco JG. Inhibition of polymorphic human carbonyl reductase 1 (CBR1) by the cardioprotectant flavonoid 7-monohydroxyethyl rutoside (monoHER). Pharm Res 2008; 25(7): 1730.*
19. *Wermuth B. Purification and properties of an NADPH-dependent carbonyl reductase from human brain. Relationship to prostaglandin 9-ketoreductase and xenobiotic ketone reductase. J Biol Chem 1981; 256(3): 1206-1213.*
20. *Pirolli D, Giardina B, Mordente A, Ficarra S, De Rosa MC. Understanding the binding of daunorubicin and doxorubicin to NADPH-dependent cytosolic reductases by computational methods. Eur J Med Chem 2012; 56: 145-154.*
21. *Krieger E, Vriend G. New ways to boost molecular dynamics simulations. J Comput Chem 2015; 36(13): 996-1007.*
22. *Malatkova P, Wsol V. Carbonyl reduction pathways in drug metabolism. Drug Metab Rev 2014; 46(1): 96-123.*
23. *Venugopala KN, Chandrashekharappa S, Pillay M, Bhandary S, Kandeel M, Mahomoodally FM, Morsy MA, Chopra D, Aldhubiab BE, Attimarad M, et al. Synthesis and structural elucidation of novel benzothiazole derivatives as anti-tubercular agents: In-silico screening for possible target identification. Med Chem 2018.*
24. *Kandeel M, Al-Taher A, Li H, Schwingenschlogl U, Al-Nazawi M. Molecular dynamics of Middle East Respiratory Syndrome Coronavirus (MERS CoV) fusion heptad repeat trimers. Comput Biol Chem 2018; 75: 205-212.*
25. *Kandeel M, Kitade Y. Molecular dynamics and binding selectivity of nucleotides and polynucleotide substrates with EIF2C2/Ago2 PAZ domain. Int J Biol Macromol 2018; 107(Pt B): 2566-2573.*
26. *Gonzalez-Covarrubias V, Kalabus JL, Blanco JG. Inhibition of polymorphic human carbonyl reductase 1 (CBR1) by the cardioprotectant flavonoid 7-monohydroxyethyl rutoside (monoHER). Pharm Res 2008; 25(7): 1730-1734.*